19), and the decrease in solvent stabilization correlates well with the average n(eff), that is, with increasing size of the attached alkyl groups.

Experimental Section

Compound Preparation. Published methods were used to prepare **1-30**. The only compounds whose preparation and properties have not been previously described[2,14] are **3-5**. They were prepared by dissolving 1,2-dimethylhydrazine dihydrochloride (Aldrich) and 2 equiv of ethyldimethylamine in 100 mL of acetonitrile/20 mmol of dihydrochloride, cooling in an ice bath, and adding acetonitrile solutions of 16 equiv of the appropriate aldehyde, followed by 0.15 mmol of sodium borohydride/mmol of aldehyde. The solution was stirred for 30 min in an ice bath after 1-2 mL of acetic acid was added dropwise and stirred at room temperature overnight. A total of 125 mL of 15% aqueous sodium hydroxide was added to the reaction mixture, and the two-phase mixture, extracted 4 times with 100 mL of pentane. Concentration and distillation gave the hydrazines.

1,2-Di-*n*-propyldimethylhydrazine (3) was obtained in 36% yield: bp 51-54 °C (15 mmHg); ^{1}H NMR ($CDCl_3$) δ 0.9 (t, 6 H), 1.5 (m, 4 H), 2.2 (s, 6 H), 2.4 (t, 4 H). The empirical formula was established by high-resolution mass spectroscopy.

1,2-Di-*n*-butyldimethylhydrazine (4) was obtained in 80% yield: bp 84-88 °C (15 mmHg); ^{1}H NMR ($CDCl_3$) δ 0.9 (t, 6 H), 1.3-1.5 (m, 8 H), 2.2 (s, 6 H), 2.4 (t, 4 H). The empirical formula was established by high-resolution mass spectroscopy.

1,2-Di-*n*-pentyldimethylhydrazine (5) was obtained in 73% yield: bp 107-111 °C (15 mmHg); ^{1}H NMR ($CDCl_3$) δ 0.9 (t, 6 H), 1.2-1.5 (m, 12 H), 2.2 (s, 6 H), 2.4 (t, 4 H). The empirical formula was established by high-resolution mass spectroscopy.

Photoelectron Spectroscopy. A Varian IEE-15 electron spectrometer has been modified with a rebuilt analyzer, Super MeGa microcomputer (CP/M operating system), and flowing He I lamp ionization source.[17] The hydrazines were introduced through a plenum chamber, using a mixture with argon as internal standard (vIP (argon) 15.76 eV; typically 30-meV peak width at half-height resolution on the instrument used). Data were transferred to an IBM-PC microcomputer via a null modem, and spectral simulations were performed on the PC, using software written by D.T.R. The PE spectra are illustrated in the thesis of D.T.R.[15]

High-Pressure Mass Spectrometry. The NBS pulsed system has been previously described.[18] For this equilibrium work, 1-5% mixtures of two hydrazines in benzene containing a trace of chloroform to scavenge anions (which increases the lifetimes of the cations being observed) were introduced into the ionization chamber at 1-2 Torr, and the parent ion concentration ratio followed until equilibrium was established. Variable-temperature data were taken on the 35 compound pairs summarized in Table VIII. Van't Hoff plots of these data appear in the thesis of D.T.R.[15] Errors in the equilibrium measurements are estimated at 0.02 eV (0.5 kcal/mol), 1 eu.

Acknowledgment. We thank the National Science Foundation for partial financial support of this work under Grant CHE-8401836.

Registry No. 1, 6415-12-9; **1**$^{+\cdot}$, 34504-32-0; **2**, 23337-93-1; **2**$^{+\cdot}$, 116149-15-6; **3**, 23337-88-4; **3**$^{+\cdot}$, 106376-61-8; **4**, 116149-14-5; **4**$^{+\cdot}$, 106376-65-2; **5**, 106376-59-4; **5**$^{+\cdot}$, 106376-60-7; **6**, 68970-05-8; **6**$^{+\cdot}$, 106376-73-2; **7**, 68970-09-2; **7**$^{+\cdot}$, 106376-68-5; **8**, 60678-73-1; **8**$^{+\cdot}$, 93473-68-8; **9**, 60678-66-2; **9**$^{+\cdot}$, 116149-16-7; **10**, 60678-72-0; **10**$^{+\cdot}$, 116149-19-0; **11**, 67092-88-0; **11**$^{+\cdot}$, 116149-17-8; **12**, 53779-90-1; **12**$^{+\cdot}$, 106403-60-5; **13**, 49840-60-0; **13**$^{+\cdot}$, 106376-71-0; **14**, 60678-76-4; **14**$^{+\cdot}$, 106376-75-4; **15**, 68970-11-6; **15**$^{+\cdot}$, 116149-20-3; **16**, 18389-95-2; **16**$^{+\cdot}$, 106376-69-6; **17**, 6130-94-5; **17**$^{+\cdot}$, 106376-72-1; **18**, 49840-66-6; **18**$^{+\cdot}$, 116149-21-4; **19**, 38704-89-1; **19**$^{+\cdot}$, 93473-70-2; **20**, 26163-37-1; **20**$^{+\cdot}$, 98705-11-4; **21**, 26171-64-2; **21**$^{+\cdot}$, 35018-93-0; **22**, 60678-80-0; **22**$^{+\cdot}$, 98719-94-9; **23**, 60678-82-2; **23**$^{+\cdot}$, 116149-18-9; **24**, 49840-68-8; **24**$^{+\cdot}$, 116149-22-5; **25**, 5397-67-1; **25**$^{+\cdot}$, 60512-67-6; **26**, 2940-98-9; **26**$^{+\cdot}$, 56894-82-7; **27**, 3661-15-2; **27**$^{+\cdot}$, 98719-78-9; **28**, 14287-89-9; **28**$^{+\cdot}$, 93601-01-5; **29**, 14287-92-4; **29**$^{+\cdot}$, 42843-04-9; **30**, 105090-34-4; **30**$^{+\cdot}$, 93601-00-4; **31**, 26163-36-0; **31**$^{+\cdot}$, 116257-44-4.

(17) We owe special thanks to A. R. DiFiore and Dr. G. Sobering for the modifications on the IEE-15.

(18) Meot-Ner (Mautner), M.; Sieck, L. W. *J. Am. Chem. Soc.* **1983**, *105*, 2596.

The Chemistry of Acetylene on the Ru(001)-p(2×2)O and Ru(001)-p(1×2)O Surfaces

J. E. Parmeter,† M. M. Hills,‡ and W. H. Weinberg*

Contribution from the Division of Chemistry and Chemical Engineering, California Institute of Technology, Pasadena, California 91125. *Received January 11, 1988*

Abstract: The chemisorption and decomposition of acetylene on Ru(001) surfaces with ordered p(2×2) and p(1×2) overlayers of oxygen adatoms has been studied by using high-resolution electron energy loss spectroscopy and thermal desorption mass spectrometry. The chemisorbed acetylene species formed on these oxygen precovered surfaces are not significantly different from molecularly chemisorbed acetylene on clean Ru(001), although one of the two types of chemisorbed acetylene formed on the clean surface is not formed on Ru(001)-p(1×2)O. The preadsorption of oxygen reduces the saturation coverages of chemisorbed acetylene, which is approximately 0.39 on clean Ru(001), 0.31 on Ru(001)-p(2×2)O, and 0.09 on Ru(001)-p(1×2)O. As on clean Ru(001), the chemisorbed acetylene on the oxygen-precovered surfaces does not desorb upon annealing but rather decomposes between 200 and 350 K to produce a number of stable intermediates, including ethylidyne (CCH_3), acetylide (CCH), methylidyne (CH), and an sp^2-hybridized vinylidene (CCH_2) species. The vinylidene is formed in particularly large amounts on Ru(001)-p(2×2)O after annealing to 350 K and appears to be stabilized strongly by the presence of coadsorbed oxygen because it is formed not at all or in trivial amounts on clean Ru(001). The stability, formation, and decomposition of the various intermediates is discussed, and the results are compared with earlier work. The decomposition of all of these intermediates leads eventually to hydrogen desorption, which is complete on both oxygen-precovered surfaces by approximately 700 K.

I. Introduction

The chemistry of acetylene on clean, single crystalline transition-metal surfaces has received a great deal of attention during the past decade.[1-4] This area of research offers both the possibility of gaining insight into industrially important catalytic reactions involving hydrocarbons and the opportunity to increase the data

† AT and T Bell Laboratories Predoctoral Fellow.
‡ Present address: Aerospace Corp., Box 92957, Los Angeles, CA 90009.

(1) Ibach, H.; Mills, D. L. *Electron Energy Loss Spectroscopy and Surface Vibrations*; Academic Press, New York, 1982; p 294.
(2) Parmeter, J. E.; Hills, M. M.; Weinberg, W. H. *J. Am. Chem. Soc.* **1986**, *108*, 3563.

0002-7863/88/1510-7952$01.50/0

base available for comparisons between the surface chemistry and the organometallic chemistry of unsaturated hydrocarbons. We have previously used high-resolution electron energy loss spectroscopy (EELS) and thermal desorption mass spectrometry (TDMS) to study the adsorption and decomposition of acetylene on clean Ru(001),[2] concluding that molecularly chemisorbed acetylene is very nearly sp^3-hybridized on this surface and that it decomposes near 250 K to produce a mixture of acetylide (CCH) and ethylidyne (CCH_3), both of which decompose between 350 and 400 K to yield methylidyne and surface carbon. The methylidyne decomposes between 500 and 700 K, and hydrogen desorbs from the surface between approximately 250 and 700 K. We have also studied the coadsorption of hydrogen and acetylene on Ru(001),[3] showing that small amounts of acetylene can be hydrogenated to ethylene via an intermediate inferred to be an sp^3-hybridized vinyl ($CHCH_2$) species.

More recently, Jakob et al.[4] have also studied acetylene adsorption on clean Ru(001) and have shown that the molecularly chemisorbed phase below 200 K consists of two species, designated Type I and Type II acetylene. The former exhibits a rather strong ν(CC) EELS loss feature near 1130 cm^{-1}, while the latter gives rise to strong CH bending loss features near 760 and 980 cm^{-1} and a much weaker ν(CC) loss feature near 1260 cm^{-1}. They also obtained a higher saturation acetylene coverage (0.43 monolayer versus our 0.27 monolayer) and reported a number of similarities and minor differences in the interpretation of acetylene decomposition. These differences are discussed in detail in Section IV.B of this paper.

The preadsorption of oxygen induces dramatic changes in the bonding of molecularly chemisorbed ethylene on several metal surfaces. On clean Pd(100),[5] Fe(111),[6] Pt(111),[7] and Ru(001),[8-10] ethylene is di-σ-bonded with rehybridization to sp^3. However, in the presence of a sufficient concentration of preadsorbed oxygen adatoms, it bonds to all of these surfaces in a π-bonded configuration, retaining its sp^2-hybridization. It is thus of interest to study the coadsorption of oxygen and acetylene on Ru(001), in order to determine whether the electron-withdrawing oxygen adatoms induce similar changes in the bonding of acetylene. The coadsorption of oxygen and acetylene has received surprisingly little attention in the past.[11] The large data base now available concerning the adsorption of ethylene[8-10,12,13] and acetylene[2-4] on clean and chemically modified Ru(001) surfaces makes this surface an ideal one on which to investigate this issue. Accordingly, we report here an EELS and TDMS study of acetylene adsorption and decomposition on two different oxygen-precovered Ru(001) surfaces. Oxygen adsorbs dissociatively on Ru(001) at 80 K, and the oxygen adatoms occupy 3-fold hollow sites exclusively.[14]

The two oxygen-precovered surfaces we have chosen to investigate are the well-characterized and reproducible Ru(001)–p(2×2)O and Ru(001)–p(1×2)O surfaces. Figure 1 shows the structures and EEL spectra of these surfaces. The p(2×2) oxygen adatom overlayer corresponds to an oxygen adatom coverage of 0.25 relative to the surface concentration of ruthenium atoms, which is 1.58×10^{15} cm^{-2}.[15] The p(1×2) oxygen adatom overlayer corresponds to an oxygen adatom coverage of 0.5, which is the saturation coverage of oxygen adatoms that can be obtained by exposing the Ru(001) surface to oxygen gas under ultrahigh vacuum (UHV) conditions. The electron-withdrawing effect of the oxygen adatoms increases the work function by 0.2 eV in the case of the p(2×2) overlayer and 1.06 eV in the case of the p(1×2) overlayer.[14] While clean Ru(001) is characterized by a featureless EEL spectrum, the ordered oxygen overlayers give rise to distinctive vibrational loss features.[16] On Ru(001)–p(2×2)O, an intense loss feature occurs at 535 cm^{-1} due to the vibration of the oxygen adatoms perpendicular to the surface, ν_s(RuO). A loss feature is also present at 250 cm^{-1} due to the coupling of the oxygen adatom vibrations to a ruthenium surface phonon. The corresponding loss features on Ru(001)–p(1×2)O occur at 585 and 240 cm^{-1}, and an additional loss feature due to the asymmetric ruthenium–oxygen stretching vibration, ν_a(RuO), occurs at 430 cm^{-1}. The latter mode involves motion of the oxygen atoms largely parallel to the surface but not entirely so due to the coupling of this mode to ν_s(RuO). It should be pointed out that the real (i.e., non-ideal) p(1×2)O overlayer actually consists of three types of independent and otherwise identical domains that are rotated 120° with respect to one another. Where these domains meet there will be small areas that are relatively oxygen-deficient and which may exhibit chemistry more typical of the p(2×2)O overlayer.

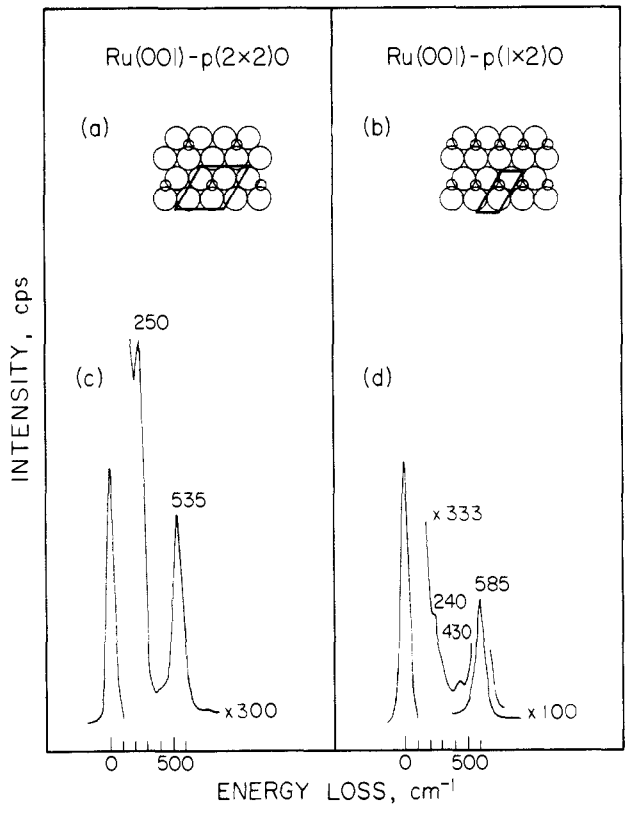

Figure 1. The structures and unit cells of (a) Ru(001)–p(2×2)O and (b) Ru(001)–p(1×2)O. Also shown are the EEL spectra corresponding to (c) the p(2×2) and (d) the p(1×2) oxygen adatom overlayers.

II. Experimental Procedures

Most of the pertinent details concerning the EEL spectrometer used in these studies and the UHV chamber housing it have been described elsewhere.[17] In our previous study of the chemistry of acetylene on clean Ru(001),[2] the thermal desorption measurements were performed in a separate UHV chamber[18] which also contains a Ru(001) crystal but

(3) Parmeter, J. E.; Hills, M. M.; Weinberg, W. H. *J. Am. Chem. Soc.* **1987**, *109*, 72.
(4) Jakob, P.; Cassuto, A.; Menzel, D. *Surface Sci.* **1987**, *187*, 407.
(5) Stuve, E. M.; Madix, R. J.; Brundle, C. R. *Surf. Sci.* **1985**, *152/153*, 532.
(6) Seip, U.; Tsai, M.-C.; Küppers, J.; Ertl, G. *Surf. Sci.* **1984**, *147*, 65.
(7) Steininger, H.; Ibach, H.; Lehwald, S. *Surf. Sci.* **1982**, *117*, 685.
(8) Barteau, M. A.; Broughton, J. Q.; Menzel, D. *Appl. Surf. Sci.* **1984**, *19*, 92.
(9) Hills, M. M.; Parmeter, J. E.; Weinberg, W. H. *J. Am. Chem. Soc.* **1987**, *109*, 597.
(10) Hills, M. M.; Parmeter, J. E.; Weinberg, W. H. *J. Am. Chem. Soc.* **1987**, *109*, 4224.
(11) Stuve, E. M.; Madix, R. J.; Sexton, B. A. *Surf. Sci.* **1982**, *123*, 491.
(12) Hills, M. M.; Parmeter, J. E.; Mullins, C. B.; Weinberg, W. H. *J. Am. Chem. Soc.* **1986**, *108*, 3554.
(13) Hills, M. M.; Parmeter, J. E.; Weinberg, W. H. *J. Am. Chem. Soc.* **1986**, *108*, 7215.
(14) Madey, T. E.; Engelhardt, H. A.; Menzel, D. *Surf. Sci.* **1975**, *48*, 304.

(15) This surface density of ruthenium atoms as well as the 1.56 Å distance between adjacent threefold hollow sites is calculated easily from the 2.71 Å nearest-neighbor distance on this surface. Kittel, C. In *Introduction to Solid State Physics*, 5th ed.; Wiley & Sons: New York, 1976; p 31.
(16) Rahman, T. S.; Anton, A. B.; Avery, N. R.; Weinberg, W. H. *Phys. Rev. Lett.* **1983**, *51*, 1979.
(17) Thomas, G. E.; Weinberg, W. H. *Rev. Sci. Instr.* **1979**, *50*, 497.
(18) Williams, E. D.; Weinberg, W. H. *Surf. Sci.* **1979**, *82*, 93.

which was more specifically designed to perform thermal desorption measurements. In this chamber, the crystal-to-mass spectrometer distance was much less than in the EELS chamber, and the mass spectrometer was interfaced to a computer which allowed the simultaneous monitoring of up to six different masses in thermal desorption spectra. The mass spectrometer in this chamber also had an attached skimmer to better distinguish desorption from the crystal face from desorption from crystal edges, support leads, etc. Since a more recent study of acetylene on Ru(001)[4] has reported qualitatively similar but quantitatively different thermal desorption results than those we obtained in our previous study, we have performed numerous additional thermal desorption measurements with acetylene in both of our UHV chambers. This has led to the conclusion that faulty computer software did indeed lead, in our previous study[2], to a calculated saturation coverage of acetylene that was too low by approximately 30%. Therefore, all of the thermal desorption measurements in the present study were performed in the same UHV chamber that houses the EEL spectrometer.

The acetylene and oxygen used in these studies, and their handling, have been discussed elsewhere, as have the cleaning and cooling of the Ru(001) crystal.[2,10]

III. Results

A. Thermal Desorption Mass Spectrometry. Following large acetylene exposures on Ru(001)–p(2×2)O and Ru(001)–p(1×2)O at 80 K, only H_2, CO, and multilayer acetylene are observed to desorb when the surface is annealed from 80 K to above 900 K. There was no detectable desorption of CH_4 or C_2H_4, for example. Multilayer acetylene adsorbs near 95 K. The acetylene multilayers were discussed in detail previously[2] and will not be considered further here.

Figure 2 shows the hydrogen (m/e = 2 amu) thermal desorption spectra that result following 5 L C_2H_2 exposures to (a) clean Ru(001), (b) Ru(001)–p(2×2)O, and (c) Ru(001)–p(1×2)O at 80 K. All of these exposures were sufficiently large to observe the sublimation of acetylenic multilayers. On all three surfaces, hydrogen desorption is complete near 700 K, and the onset of desorption is near 250 K on clean Ru(001), near 215 K on Ru(001)–p(2×2)O, and near 300 K on Ru(001)–p(1×2)O. Each spectrum shows a relative minimum in the rate of H_2 evolution near 450–480 K, and the percentage of H_2 desorbing below this minimum is estimated to be approximately 55–60% on clean Ru(001), 45–50% on Ru(001)–p(2×2)O, and 20–40% on Ru(001)–p(1×2)O. Note that the value for clean Ru(001) is lower than our previously published value of 75%.[2]

The saturation coverage of acetylene on each surface following adsorption at 80 K was estimated by comparing the integrated intensities of the thermal desorption spectra of Figure 2 with the integrated intensities of H_2 thermal desorption spectra measured following saturation (10 L) hydrogen exposures to clean Ru(001) (the latter of which were obtained immediately prior to the oxygen and acetylene exposures). For clean Ru(001), a saturation hydrogen adatom coverage of 0.85 was assumed in accordance with the previously published value of Shimizu et al.[19] The resulting saturation acetylene coverages, which are accurate to approximately ±0.05 monolayer, are 0.39 monolayer on clean Ru(001), 0.31 monolayer on Ru(001)–p(2×2)O, and 0.09 monolayer on Ru(001)–p(1×2)O. Note that the value of 0.39 on clean Ru(001) is higher than our previously published value of 0.27,[2] which we now believe to be in error. Note also that our coverages must be multiplied by 1/0.85 = 1.18 in order to be compared directly to the clean surface coverage in ref 4, since a saturation hydrogen adatom coverage of unity was assumed in that study.

Following exposures of acetylene on Ru(001)–p(2×2)O and Ru(001)–p(1×2)O, the desorption of carbon monoxide was also observed due to the recombination of carbon (formed from acetylene decomposition) and oxygen adatoms. This desorption occurred between approximately 450 and 780 K on both surfaces, with a peak desorption temperature of approximately 620 K. Since the relative uncertainty in our determination of the saturation acetylene coverage on Ru(001)–p(1×2)O with hydrogen thermal desorption is quite large (0.09 ± 0.05), we attempted to measure the amount of CO desorbed from this surface following a saturation acetylene exposure. Since a sloping background is always present in mass 28 thermal desorption spectra obtained in our chamber due to the presence of CO in the chamber background, and since the recombinatively desorbed CO desorbs over a broad temperature range, this estimate is rather crude. However, a reasonable base line could be obtained by performing a mass 28 thermal desorption spectrum after exposing the *clean* Ru(001) surface to a saturation acetylene exposure at 80 K (where no recombinative CO desorption occurs) and subtracting this base line from the mass 28 thermal desorption spectrum for C_2H_2 on Ru(001)–p(1×2)O. The remaining integrated intensity was compared to that obtained for a mass 28 thermal desorption spectrum following a saturation CO exposure on clean Ru(001) at room temperature, where the carbon monoxide coverage is known to be approximately 0.68.[20] The result obtained is that approximately 0.17 monolayer of CO desorbs recombinatively, corresponding to an acetylene coverage of approximately 0.08, in very good agreement with the H_2 thermal desorption result.

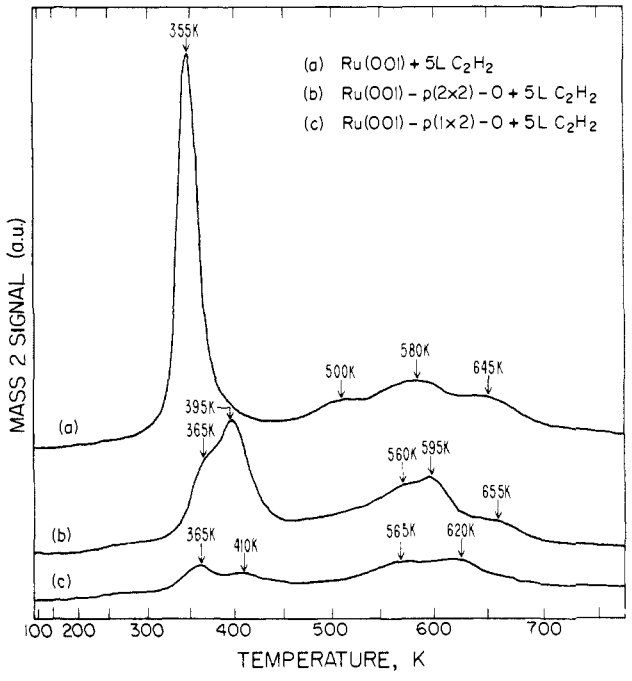

Figure 2. The H_2 (m/e = 2 amu) thermal desorption spectra that result following a 5 L C_2H_2 exposure to (a) clean Ru(001), (b) Ru(001)–p(2×2)O and (c) Ru(001)–p(1×2)O at 80 K. The heating rate was approximately 10 K-s^{-1} in all cases. The three spectra are only approximately to scale with respect to one another; each one was calibrated separately against a saturation H_2 exposure.

B. Electron Energy Loss Spectroscopy. i. Molecularly Chemisorbed Acetylene on Ru(001)–p(2×2)O. Figure 3 shows the EEL spectra that result when the Ru(001)–p(2×2)O surface at 80 K is exposed to (a) 0.2 L C_2H_2, (b) 2 L C_2H_2, and (c) 2 L C_2D_2. The spectrum of Figure 3a is dominated by Type I acetylene and is similar to previous results obtained for low coverages of chemisorbed acetylene on clean Ru(001),[4] with the dominant loss features being ν(CC) (1110 cm^{-1}) and ν(CH) (2990 cm^{-1}). The frequencies of these modes are very similar to their clean surface values, with ν(CH) being slightly (approximately 40 cm^{-1}) upshifted. The weak shoulder that is present at 730 cm^{-1} indicates the presence of a very small amount of Type II acetylene as well. At a near saturation exposure [cf. Figure 3b], much more Type II acetylene is clearly present, as evidenced by the CH bending loss features at 740 and 960 cm^{-1}. The EEL spectrum of Figure 3b is very similar to that obtained for a saturation acetylene exposure on Ru(001) at 80 K followed by annealing to 150 K.[2] The shoulders near 420 and 470 cm^{-1} in Figure 3 (parts a and b) probably derive intensity mainly from the RuC stretching

(19) Shimizu, H.; Christmann, K.; Ertl, G. *J. Catal.* **1980**, *61*, 412.

(20) Pfnür, H.; Menzel, D.; Hoffmann, F. M.; Ortega, A.; Bradshaw, A. M. *Surf. Sci.* **1980**, *93*, 431.

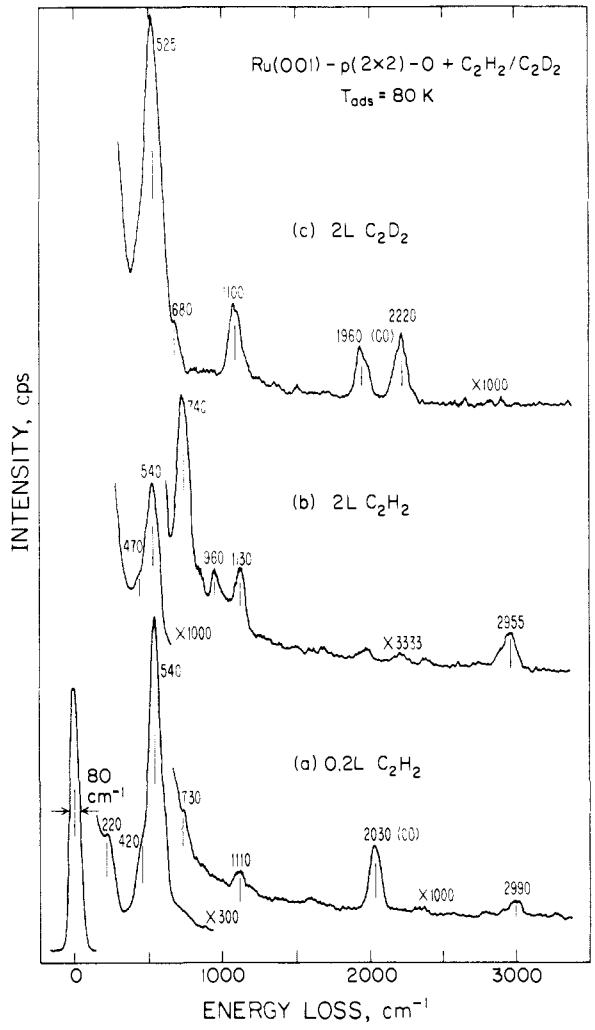

Figure 3. The EEL spectra obtained following the exposure of acetylene to Ru(001)–p(2×2)O at 80 K. The exposures are (a) 0.2 L C_2H_2, (b) 2 L C_2H_2, and (c) 2 L C_2D_2.

modes of the chemisorbed acetylene, although contributions from ν_a(RuO) due to p(1×2)-like defects in the p(2×2)O overlayer cannot be excluded in (b).[16] The EEL spectrum of Figure 3c is due to a near saturation coverage of deuteriated acetylene on Ru(001)–p(2×2)O and again clearly shows a mixture of Type I [ν(CC) = 1100 cm^{-1}] and Type II [CD bend as a shoulder at 680 cm^{-1}, downshifted from 960 cm^{-1} in C_2H_2] acetylene. The strong CD bend of the Type II acetylene is downshifted from 740 cm^{-1} in C_2H_2 to approximately 565 cm^{-1},[2,4] overlapping with the ν_s(RuO) and ν(RuC) loss features and forming a broad feature centered at 525 cm^{-1}. As with C_2H_2, the frequencies of the observed loss features for both types of C_2D_2 are shifted very slightly, or not at all, compared to the clean surface.

It should be noted that the relative amounts of Type I and Type II acetylene formed on Ru(001)–p(2×2)O following a saturation C_2H_2 exposure at 80 K were found to be somewhat variable. The intensity of the Type I acetylene ν(CC) loss feature at 1130 cm^{-1} varied from being approximately as intense as the Type II CH bending mode at 960 cm^{-1} [as in Figure 3b] to only about a third as intense in some other spectra. The latter probably correspond to surfaces with oxygen adatom coverages slightly greater than 0.25, so that small areas of the surface have a p(1×2)O rather than a p(2×2)O structure. The formation of a complete p(1×2)O overlayer blocks the formation of Type I acetylene completely (cf. Section III.B.ii).

The chemisorbed acetylene on Ru(001)–p(2×2)O is stable below 200 K, beginning to decompose in the temperature range between 200 and 250 K. Thus, the chemisorbed acetylene is not stabilized compared to the clean surface, where decomposition begins near 230 K.[2]

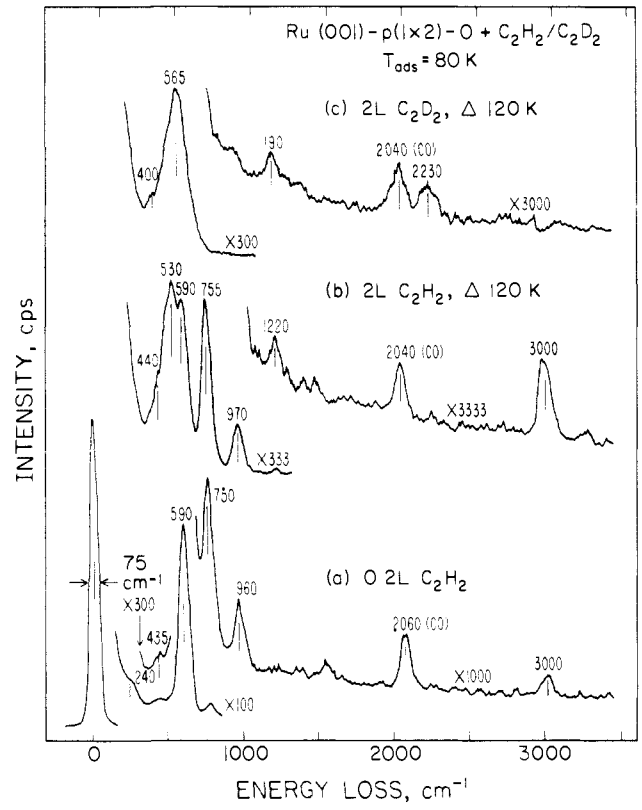

Figure 4. The EEL spectra obtained following the adsorption of acetylene on Ru(001)–p(1×2)O at 80 K. The exposures are (a) 0.2 L C_2H_2, (b) 2 L C_2H_2, and (c) 2 L C_2D_2. In (b) and (c) the surface was annealed briefly to 120 K following acetylene adsorption in order to remove small amounts of multilayer acetylene.

ii. Molecularly Chemisorbed Acetylene on Ru(001)–p(1×2)O. Electron energy loss spectra of acetylene adsorbed on Ru(001)–p(1×2)O are shown in Figure 4. The most prominent result, evident in Figure 4a, is that even for very low coverages, only Type II acetylene is formed, as evidenced by the lack of the characteristic ν(CC) loss feature near 1130 cm^{-1} of Type I acetylene.[4] Occasionally, a very weak peak was observed near 1130 cm^{-1} (approximately one-tenth as intense as the 960 cm^{-1} loss feature of Type II acetylene), due, presumably, to an oxygen adatom coverage of slightly less than the ideal p(1×2) coverage of 0.5 or to the formation of Type I acetylene at p(1×2)O domain boundaries.

The spectrum of Figure 4b corresponds to a saturation coverage of C_2H_2 on Ru(001)–p(1×2)O. The surface was annealed briefly to 120 K following acetylene adsorption at 80 K in order to desorb small amounts of multilayer acetylene. Again, only Type II acetylene is present, displaying the characteristic CH bending modes at 755 and 970 cm^{-1} and ν(CH) at 3000 cm^{-1}. The carbon–carbon stretch is also resolved as a weak loss feature at 1220 cm^{-1}. We were not able to resolve this loss feature on clean Ru(001) or Ru(001)–p(2×2)O, most likely due to overlap with the ν(CC) loss feature of Type I acetylene, but the frequency observed here is quite close to the frequency of 1260 cm^{-1} reported by Jakob et al. for clean Ru(001).[4] Finally, there is a very intense loss feature at 530 cm^{-1} which is tentatively assigned as a ruthenium–carbon stretching mode of the adsorbed acetylene. Similar frequencies have been observed for this mode on clean Ru(001),[2,4] although this loss feature was not nearly so intense in those cases.

Figure 4c shows the EEL spectrum that results when the Ru(001)–p(1×2)O surface is exposed to 2 L of C_2D_2 at 80 K, followed by annealing to 120 K to remove any multilayer acetylene. The only loss features of the chemisorbed acetylene that are resolved clearly are ν(CD) at 2230 cm^{-1} and ν(CC) at 1190 cm^{-1}, which are due to Type II acetylene. The downshifted CD bending modes, the RuC stretching modes, and the ν_s(RuO) mode all

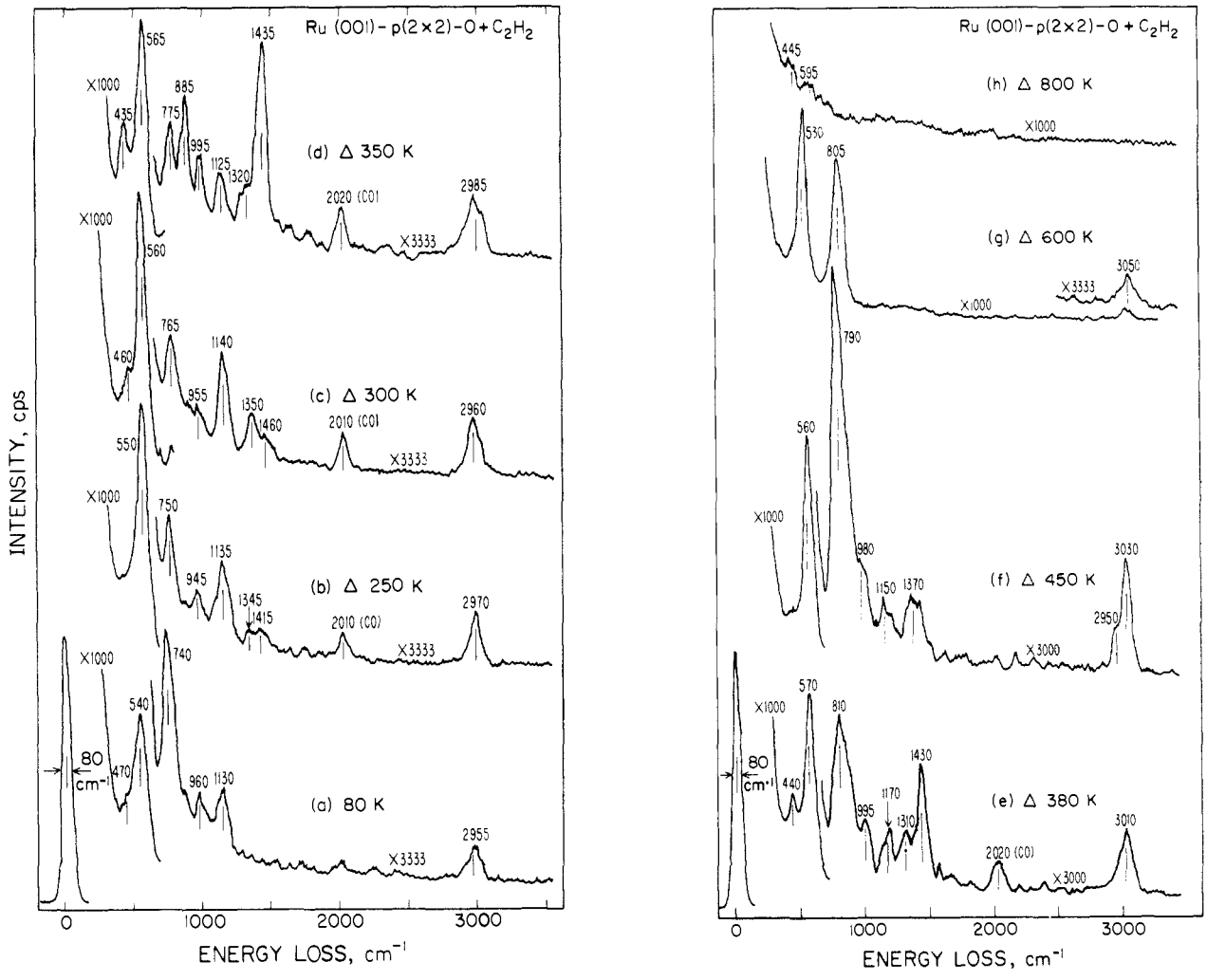

Figure 5. Electron energy loss spectra showing the thermal decomposition of acetylene (C_2H_2) on Ru(001)–p(2×2)O. The annealing temperatures are (a) 80, (b) 250, (c) 300, (d) 350, (e) 380, (f) 450, (g) 600, and (h) 800 K. The exposure was of 2 L C_2H_2 at 80 K.

overlap, forming a broad loss feature centered at 565 cm^{-1}.

Both EELS and TDMS results indicate that chemisorbed acetylene begins to decompose near 300 K on Ru(001)–p(1×2)O. It is thus stabilized significantly compared to the clean Ru(001) surface.

iii. Decomposition of Chemisorbed Acetylene on Ru(001)–p-(2×2)O. A series of EEL spectra obtained following the adsorption of 2 L of C_2H_2 on Ru(001)–p(2×2)O at 80 K followed by annealing to various temperatures is shown in Figure 5. In the discussion that follows, it is useful to refer to Table I, which summarizes the vibrational spectra of species identified previously in the decomposition of acetylene and ethylene on various Ru(001) surfaces.[2-4,8-13] As noted previously, decomposition begins between 200 and 250 K, and annealing from 80 to 250 K causes several changes in the EEL spectrum. The loss features due to Type II acetylene decrease in intensity, the loss feature near 1135 cm^{-1} increases in intensity, and new loss features appear at 1345 and 1415 cm^{-1}. The loss feature at 1345 cm^{-1} and the increase in intensity of the 1135-cm^{-1} loss feature are attributed to $\delta_s(CH_3)$ and $\nu(CC)$ of ethylidyne. Since ethylidyne (CCH_3) contains more hydrogen atoms than acetylene, a dehydrogenation product must also be present. Indeed, acetylide (CCH) is present but cannot be unambigously resolved in Figure 5b because its characteristic CH bending loss feature occurs at nearly the same frequency (approximately 750 cm^{-1}) as the intense CH bend of Type II acetylene. Finally, the loss feature at 1415 cm^{-1} is due in part to $\delta_a(CH_3)$ of ethylidyne, although its intensity suggests the presence of a $\delta(CH_2)$ mode due either to a vinyl ($CHCH_2$) or, more likely, to a vinylidene (CCH_2) species. Note that little, if any, Type I acetylene has decomposed by 250 K. Annealing to 300 K results in the formation of additional ethylidyne and a strong decrease in the intensity of the Type II acetylene CH bending mode near 955 cm^{-1}, which indicates clearly that the 765 cm^{-1} loss feature of Figure 5c is due primarily to acetylide rather than Type II acetylene.

Table I. Vibrational Frequencies (in cm^{-1}) of Various Hydrocarbon Intermediates[a,b]

species	mode	frequency
(1) ethylidyne (CCH_3)	$\nu_a(CH_3)$	3000–3045 vw
	$\nu_s(CH_3)$	2910–2970 s
	$\delta_a(CH_3)$	1440–1450 w
	$\delta_s(CH_3)$	1340–1370 s
	$\nu(CC)$	1120–1140 s
	$\rho(CH_3)$	970–1000 w
	T_z	450–480 w
(2) vinylidene (CCH_2)	$\nu_a(CH_2)$	3050 w
	$\nu_s(CH_2)$	2985 m
	$\nu(CC) + \delta(CH_2)$	1435 vs
	$\rho(CH_2)$	965 w
	$\omega(CH_2)$	895 s
	T_z	455 s
(3) acetylide (CCH)	$\nu(CH)$	2935–2960 w
	$\nu(CC)$	1290 w
	$\delta(CH)$	750–770 s
	T_z	435 m
(4) methylidyne (CH)	$\nu(CH)$	3010–3030 w
	$\delta(CH)$	800–840 s
	T_z	440–550 m

[a] s = strong, m = medium, w = weak, v = very. [b] Identified previously in the decomposition of acetylene and ethylene on clean and/or chemically modified Ru(001) surfaces. This is a summary of data from ref 2–4 and 8–13.

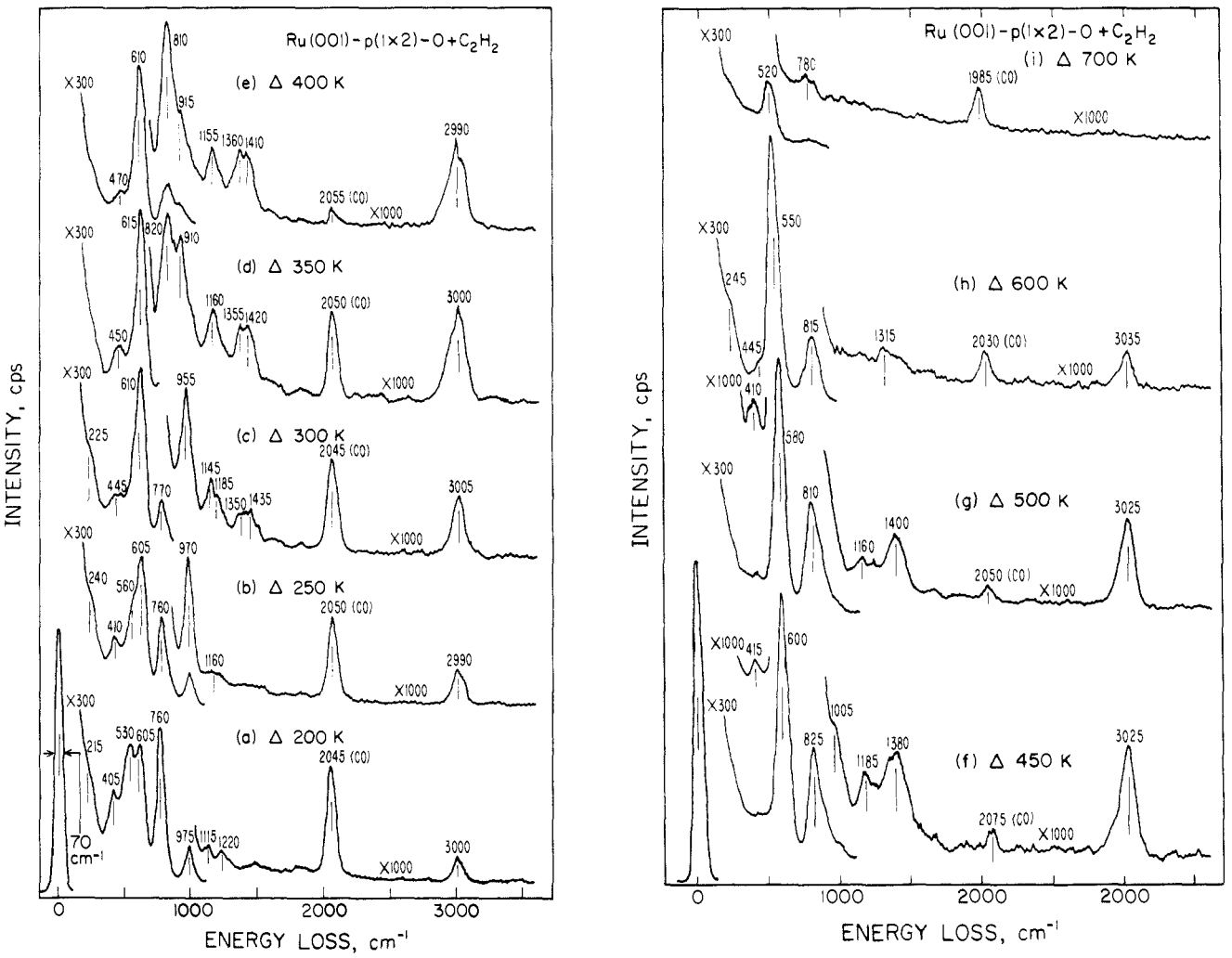

Figure 6. Electron energy loss spectra showing the thermal decomposition of acetylene (C_2H_2) on Ru(001)–p(1×2)O. The annealing temperatures are (a) 200, (b) 250, (c) 300, (d) 350, (e) 400, (f) 450, (g) 500, (h) 600, and (i) 700 K. The exposure was of 4 L C_2H_2 at 80 K.

Much more pronounced changes occur when the surface is annealed from 300 to 350 K. Strong loss features appear at 1435, 885, and 435 cm^{-1} which are due to the formation of an sp^2-hybridized vinylidene species which we have identified previously as a decomposition product of ethylene on Ru(001)–p(2×2)O.[9,10] The mode assignments are ν(CC) and $\delta(CH_2)$ (uncoupled), 1435 cm^{-1}; $\omega(CH_2)$, 885 cm^{-1}; and ν(Ru–CCH_2), 435 cm^{-1}. Some ethylidyne is also present as evidenced by the loss features at 1125 and 1320 cm^{-1}, and, in fact, the amount of ethylidyne seems to be reduced only slightly compared to the 300 K spectrum, as evidenced by the intensity of the latter mode. The loss feature at 775 cm^{-1} is due to δ(CH) of acetylide. The 995-cm^{-1} loss feature is more problematic; both vinylidene [$\rho(CH_2)$] and ethylidyne [$\rho(CH_3)$] have loss features that occur near this frequency, but both of these modes are usually quite weak. It appears that virtually all of the chemisorbed acetylene has decomposed by 350 K. The 955-cm^{-1} loss feature of Type II acetylene has disappeared completely, and the decomposition of Type I acetylene is indicated by the large decrease in the intensity of the loss feature near 1140 cm^{-1} upon annealing from 300 to 350 K. It is interesting to note that the decomposition of the Type I acetylene correlates with the appearance of the strong modes due to sp^2-hybridized vinylidene.

Annealing to 380 K results in the decomposition of much of the vinylidene, an upshift in the center of the peak near 3000 cm^{-1} due to CH stretching modes, and the development of a broad loss feature centered at 810 cm^{-1}. The last feature grows in intensity upon annealing to 450 K, while all of the loss features due to vinylidene disappear, and loss features remain at 980, 1150, and 1370 cm^{-1}. While these last three modes are due primarily to ethylidyne, they are quite broad, and contributions from the carbon–carbon stretching vibrations of C_2 dimers or other forms of surface carbon cannot be excluded.[4,12] In fact, a corresponding EEL spectrum for C_2D_2 on Ru(001)–p(2×2)O annealed to 450 K shows a broad, weak loss feature at 1315 cm^{-1} due to some type of carbon–carbon stretching mode(s). Annealing to 600 K leaves only the ν_s(RuO) loss feature at 530 cm^{-1}, the loss feature at 805 cm^{-1} (now rather sharp), and a CH stretching loss feature at 3050 cm^{-1}. The loss features at 805 and 3050 cm^{-1} have been assigned previously to the δ(CH) and ν(CH) modes, respectively, of an inclined methylidyne (CH) species.[2,8,12]

Finally, annealing to 800 K causes all of the methylidyne to decompose and the oxygen to be titrated away [as CO(g)] by surface carbon, leaving very weak loss features near 445 and 595 cm^{-1} which are due to surface carbon. These EELS results are in good qualitative agreement with the thermal desorption results, of which the latter show the desorption of H_2 to be complete near 700 K.

iv. Decomposition of Chemisorbed Acetylene on Ru(001)–p(1×2)O. The decomposition of acetylene on Ru(001)–p(1×2)O was also investigated, and a series of EEL spectra obtained following a 4 L exposure at 80 K with annealing to various temperatures is shown in Figure 6. It is clear from inspection of Figure 6 that many of the same decomposition products occur that are formed on Ru(001)–p(2×2)O, and we note here only some of the more interesting differences.

Probably the most striking difference is that much less sp^2-hybridized vinylidene is formed than on Ru(001)–p(2×2)O. In the 350 K EEL spectrum [Figure 6d], loss features are present at 1420, 910, and 450 cm^{-1} which can be attributed entirely or in part to this species, but in comparison to the remaining loss features in the spectrum these are much less intense than the

Table II. Vibrational Frequencies (in cm^{-1}) of Molecularly Chemisorbed Acetylene on Ru(001), Ru(001)–p(2×2)O, and Ru(001)–p(1×2)O

acetylene loss features		clean Ru(001) (2)	clean Ru(001) (4)	Ru(001)–p(2×2)O (this work)	Ru(001)–p(1×2)O (this work)
Type I	ν(CH)	n.o.[a]	2950	2990	present not at all or in trivial amounts[b]
	ν(CC)	1135	1110	1110–1130	
Type II	ν(CH)	2940	2950	2955	3000
	ν(CC)	n.o.[a]	1260	n.o.[a]	1220
	CH bends	980	975	960	960
		765	740	740	750
	ν(RuC)	520	540	n.o.[a]	530
		375	370	n.o.[a]	n.o.[a]

[a] n.o. = not observed. [b] When very small amounts are present, ν(CC) = 1115.

corresponding ones in Figure 5d. The fact that virtually no Type I acetylene is formed on Ru(001)–p(1×2)O [although a trivial amount is present in Figure 6a as evidenced by ν(CC) at 1115 cm^{-1}] tends to support the observation that on Ru(001)–p(2×2)O most of the sp^2-hybridized vinylidene is formed via decomposition of Type I acetylene rather than Type II acetylene.

Apart from this obvious difference, the spectra are similar to those of Figure 5 in many respects, although on Ru(001)–p(1×2)O no decomposition products appear at 250 K, again suggesting that the chemisorbed acetylene is stabilized slightly on this surface. Ethylidyne is clearly formed on both surfaces and in each case at least some appears to be stable to 450 K. The spectra obtained following annealing to 450 and 600 K on both oxygen-precovered surfaces are very similar indeed, the only notable difference being the presence of a broad loss feature near 1315 cm^{-1} in Figure 6h that is not apparent in Figure 5g. This feature is attributed to carbon–carbon stretching modes of some form of surface carbon.[4,12]

IV. Discussion

A. Molecularly Chemisorbed Acetylene. Table II lists the frequencies of various vibrational loss features of chemisorbed Type I and Type II acetylene on clean Ru(001), Ru(001)–p(2×2)O, and Ru(001)–p(1×2)O. It is immediately apparent that ordered oxygen overlayers do not significantly affect the vibrational spectra of either type of acetylene on Ru(001). The only frequency shift that is large enough to have any significance and which appears to be reproducible is the upshift of the ν(CH) frequency of Type II acetylene to 3000 cm^{-1} on Ru(001)–p(1×2)O, which is approximately 60 cm^{-1} higher than its clean surface value. However, this does not seem to indicate a rehybridization of the Type II acetylene toward sp^2, since the ν(CC) frequency we measure is slightly *lower* than that reported by Jakob et al. on clean Ru(001).[4] It can be concluded that the structure and bonding of acetylene on the oxygen-precovered surfaces is virtually identical with the structure and bonding on the clean surface and that the electron-withdrawing effect of the oxygen has a negligible influence on these properties. The low ν(CC) frequencies of approximately 1135 cm^{-1} for Type I acetylene and 1220 cm^{-1} for Type II acetylene indicate clearly that the molecularly chemisorbed acetylene is essentially sp^3-hybridized.

It was found that the preadsorption of oxygen inhibits the adsorption of acetylene on Ru(001), with the p(2×2)O overlayer reducing the saturation coverage by approximately 20% and the p(1×2)O overlayer reducing it by approximately 75% compared to the clean surface. This coverage reduction could be due both to steric and to electronic effects of the preadsorbed oxygen. The fact that the vibrational spectra of chemisorbed acetylene are not changed significantly in the presence of oxygen suggests that steric (i.e., site-blocking) effects are of primary importance, and in fact the lack of formation of Type I acetylene on Ru(001)–p(1×2)O can be explained in terms of a site-blocking argument based on the previously proposed adsorption sites of Type I and Type II acetylene.[4] The Type I acetylene is believed to occupy μ-sites and

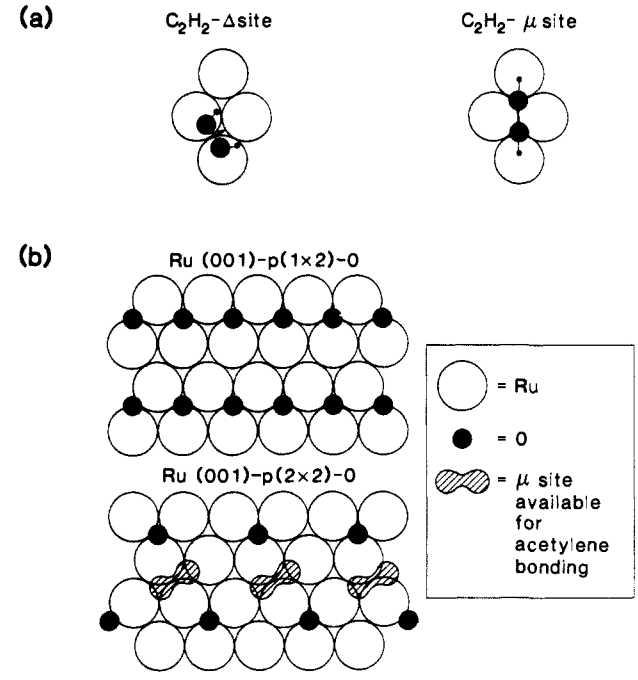

Figure 7. (a) Illustration of the previously proposed bonding sites (4) for Type I (μ-site) and Type II (Δ-site) acetylene on Ru(001). (b) The structures of Ru(001)–p(1×2)O and Ru(001)–p(2×2)O. Assuming that the acetylene carbon atoms cannot occupy 3-fold sites directly adjacent to those occupied by oxygen adatoms, μ-site bonding is possible on Ru(001)–p(2×2)O but not on Ru(001)–p(1×2)O.

the Type II acetylene Δ-sites, as shown in Figure 7. It can be seen that in the μ-type bonding the two carbon atoms of acetylene occupy adjacent 3-fold hollow sites, which on Ru(001) are located 1.56 Å apart.[15] It is reasonable to assume that a preadsorbed oxygen adatom blocks the adsorption of acetylene into the three adjacent 3-fold hollow sites since the site separation distance of 1.56 Å is only slightly longer than a CO single-order bond length and shorter than the sum of the covalent radii of an oxygen atom and a CH group. Hence, the formation of Type I acetylene is possible on Ru(001)–p(2×2)O up to a maximum coverage of θ (Type I) = 0.25. However, on Ru(001)–p(1×2)O there do not exist two adjacent 3-fold hollow sites neither of which is directly adjacent to a 3-fold hollow site already occupied by an oxygen adatom, and thus *Type I bonding is not possible.* On the other hand, Δ-type bonding involves essentially bonding of the entire acetylene molecule over a single 3-fold hollow site and is thus possible on both Ru(001)–p(2×2)O and Ru(001)–p(1×2)O. We therefore believe that the EELS evidence concerning the lack of Type I acetylene formation on Ru(001)–p(1×2)O provides support for the previously proposed bonding geometries of Type I and Type II acetylene. It must also be pointed out, however, that site-blocking arguments alone cannot explain the low saturation coverage of acetylene on Ru(001)–p(1×2)O, since enough 3-fold hollow sites not adjacent to oxygen atoms are still present on this surface to form up to a quarter monolayer of Type II acetylene. (There are actually a half monolayer of such 3-fold sites, but it is sterically possible only to put an acetylene molecule at half of these.) The saturation acetylene coverage of 0.09 monolayer must therefore be influenced by some electronic effect, e.g., by a reduction in the local density of states at the Fermi level due to the electrons "tied-up" in ruthenium–oxygen bonding, making less electron density available for ruthenium–acetylene bonding.

Another possible explanation for the low saturation acetylene coverage on Ru(001)–p(1×2)O is that acetylene adsorption could be limited to p(1×2) domain boundaries that are relatively oxygen-deficient and thus are similar to small areas of p(2×2)O structure on the surface. This would suggest that no acetylene adsorption and decomposition would be observed on a hypothetical, perfect Ru(001)–p(1×2)O surface, for either steric or electronic reasons. If this is the case, the lack of Type I acetylene on the

Ru(001)–p(1×2)O surface is still qualitatively understandable, since it would be unlikely to have two of the adjacent, available 3-fold hollow sites in the small regions defining the domain boundaries.

It is interesting to compare the bonding of molecularly chemisorbed ethylene and acetylene on clean and oxygen-precovered Ru(001) surfaces. On clean Ru(001), ethylene is rehybridized to sp^3 in a di-σ-bonded configuration,[8,12] while on Ru(001)–p-(2×2)O[9,10] and Ru(001)–p(1×2)O[8-10] it forms an sp^2-hybridized, π-bonded species. Acetylene, on the other hand, forms the same two species on clean Ru(001) and Ru(001)–p(2×2)O, and while one of these (Type I acetylene) is not formed on Ru(001)–p-(1×2)O due to geometric effects, the bonding of Type II acetylene (and its vibrational spectrum) is virtually identical with its bonding (and vibrational spectrum) on the other two surfaces. The fact that ethylene is approximately sp^2-hybridized on the oxygen-precovered surfaces, while acetylene is nearly sp^3-hybridized, probably results from the differing energies of the π^* orbitals of ethylene and acetylene. The Fermi levels of the Ru(001), Ru-(001)–p(2×2)O, and Ru(001)–p(1×2)O surfaces lie approximately 5.5, 5.7, and 6.6 eV below the vacuum level, respectively.[21,14] The unoccupied π^* orbitals of gas-phase ethylene ($1b_{2g}$) and acetylene (π_g) lie at −2.85 and −6.1 eV with respect to the vacuum level, respectively.[22,13] Upon adsorption, these orbital energies will downshift and broaden,[24] but the π^* orbital of ethylene should still lie substantially above the Fermi levels of the three ruthenium surfaces, making electron backdonation from the metal 5d band difficult, especially on the oxygen-precovered surfaces, and resulting in only minor rehybridization of the ethylene on these two surfaces. On the other hand, the π^* orbitals of chemisorbed acetylene will lie near or below the Fermi levels of all three ruthenium surfaces, so that strong rehybridization occurs even on Ru(001)–p(1×2)O.

B. Decomposition of Molecularly Chemisorbed Acetylene. The decomposition of molecularly chemisorbed acetylene has now been studied on clean Ru(001),[2,4] Ru(001)–p(2×2)O and Ru(001)–p(1×2)O. The discussion presented here will consider separately the different intermediates that are observed and will address related issues for all three surfaces.

i. Acetylide (CCH). Since studies of acetylene decomposition on the three ruthenium surfaces cited above have been made primarily for saturation coverages and under UHV conditions where adsorption of residual hydrogen should be negligible, and since in any case hydrogen does not chemisorb on the two oxygen-precovered surfaces at the temperatures where acetylene decomposition begins, the hydrogen atoms that are needed to produce ethylidyne from acetylene must be provided by the decomposition of other acetylene molecules. On clean Ru(001), the source of this hydrogen appears to be almost entirely carbon–hydrogen bond cleavage to produce acetylide, i.e.,

$$C_2H_2(a) \rightarrow CCH(a) + H(a)$$

The acetylide has also been identified in the case of ethylene decomposition on Ru(001)[12] and is characterized principally by a strong bending mode, δ(CH), at approximately 750 cm^{-1}. Its remaining vibrational loss features, ν(CC) at 1290 cm^{-1} and ν(CH) at 2960 cm^{-1}, are often obscured by the presence of loss features due to other surface species.

On all ruthenium surfaces studied, the temperature at which acetylide begins to form would appear to be identical with that where acetylene decomposition begins, namely between 200 and 250 K on clean Ru(001) and Ru(001)–p(2×2)O and near 300 K on Ru(001)–p(1×2)O. The decomposition of acetylide formed from acetylene decomposition on clean Ru(001) has been reported to be complete by 380[2] or 450 K,[4] although this discrepancy is due to differing interpretations of the upshift in the prominent δ(CH) mode that occurs near 400 K [cf. Section IV.B.iv]. Since acetylide appears to be more stable than ethylidyne and vinylidene on clean Ru(001), we do not believe that it is likely to be an intermediate in the formation of those species.

ii. Vinylidene (CCH_2). We have shown that annealing an acetylene-saturated Ru(001)–p(2×2)O surface to 350 K leads to the formation of substantial amounts of an sp^2-hybridized vinylidene species, characterized primarily by intense loss features at 1435 [ν(CC) + $\delta(CH_2)$], 885 [$\omega(CH_2)$], and 435 [ν(Ru-CCH_2)] cm^{-1}. The same species is formed on Ru(001)–p(2×2)O as the result of ethylene decomposition.[9,10] It has begun to decompose by 380 K and appears to be gone entirely by 450 K, and its disappearance correlates with the formation of an intense δ(CH) mode near 800 cm^{-1}. Its appearance correlates with the decomposition of Type I acetylene, but the mechanism of the (probably not elementary) reaction

$$C_2H_2 \text{ (Type I)} \rightarrow sp^2\text{-}CCH_2$$

is not known. We regard a direct 1,2-hydrogen transfer reaction as unlikely, since the strained geometry of the [C···H···C] transition state would probably result in a larger activation barrier than that which would be present for stepwise C–H bond formation and bond cleavage.

Small concentrations of a species that gives rise to a $\delta(CH_2)$ mode appear to be present following acetylene adsorption on Ru(001)–p(2×2)O and annealing to 250 K and on Ru(001)–p-(1×2)O at least in the temperature range of 300–400 K. The species involved is probably also vinylidene, although the presence of a vinyl ($CHCH_2$) species cannot be ruled out. We stress once again that the presence of relatively little vinylidene in the decomposition of acetylene on Ru(001)–p(1×2)O, as judged from the relatively low intensity of the 1410–1435 cm^{-1} loss feature compared to the other loss features, is strong supporting evidence for the proposition that it is primarily Type I acetylene that gives rise to vinylidene formation on Ru(001)–p(2×2)O.

On clean Ru(001) there has been some disagreement concerning the formation of vinylidene in acetylene decomposition. Ethylidyne (cf. Section IV.B.iii) formed from acetylene on clean Ru(001) gives rise to loss features near 1140, 1360, and 1440 cm^{-1}, and based on changes in the relative intensities of these loss features between 300 and 350 K Jakob et al.[4] concluded that another surface species was present and contributing to the intensity of the 1140 and 1440 cm^{-1} loss features. This species was identified as vinylidene, with $\delta(CH_2)$ at 1440 cm^{-1} and $\omega(CH_2)$ at 1140 cm^{-1}. On the other hand, we do not believe that our own data on clean Ru(001) for annealing temperatures between 230 and 350 K justify the conclusion that any species other than acetylide and ethylidyne is present. We cannot rule out, however, the presence of small amounts of vinylidene on clean Ru(001). We believe the spectrum of Figure 5d indicates clearly that the amount of vinylidene present due to acetylene decomposition on clean Ru(001) is indeed very small, since on the clean surface the 1440 cm^{-1} loss feature never has much greater intensity than the 1360 cm^{-1} loss feature. We also believe that *any* vinylidene formed on clean Ru(001) would more likely be sp^3-hybridized than sp^2-hybridized, just as ethylene is sp^3-hybridized on clean Ru(001) but sp^2-hybridized on the oxygen-precovered ruthenium surfaces. An sp^3-hybridized vinylidene species on clean Ru(001) would indeed be expected to have a CH_2 wagging frequency near 1200 cm^{-1}, rather than near 900 cm^{-1} as in the case of sp^2-hybridized vinylidene.[25]

In summary, the p(2×2) oxygen adatom overlayer enhances substantially the stability of sp^2-hybridized vinylidene on Ru(001), whether formed from ethylene or acetylene decomposition.

iii. Ethylidyne (CCH_3). Ethylidyne is formed as a decomposition product of acetylene on clean Ru(001),[2,4] Ru(001)–p(2×2)O, and Ru(001)–p(1×2)O. It is characterized primarily by two loss features of approximately equal intensity, $\delta_s(CH_3)$ at approximately 1360 cm^{-1} and ν(CC) at approximately 1140 cm^{-1}. On Ru(001)–p(2×2)O it appears at an annealing temperature of approximately 250 K, reaches its maximum concentration by about 300 K, and has completely decomposed by about 500 K.

(21) Wandelt, K.; Hulse, J.; Küppers, J. *Surf. Sci.* **1981**, *104*, 212.
(22) Mulliken, R. S. *J. Chem. Phys.* **1979**, *71*, 556.
(23) Dance, D. F.; Walker, I. C. *Chem. Phys. Lett.* **1973**, *18*, 601.
(24) Demuth, J. E.; Eastman, D. E. *Phys. Rev. B* **1976**, *13*, 1523.
(25) Reference 1, p 195.

The corresponding temperatures on Ru(001)-p(1×2)O are approximately 300, 350, and 500 K, although the latter is difficult to judge due to the presence of carbon–carbon stretching loss features in the 1000–1400-cm^{-1} regime at elevated temperatures. Ethylidyne is thus stabilized on the oxygen precovered surfaces compared to clean Ru(001), where it has decomposed completely by about 360–370 K.[2,4,8,10]

Our previous results[2] and those of Jakob et al.[4] are slightly different regarding the temperature of ethylidyne formation from acetylene decomposition on clean Ru(001). We found that adsorption of a saturation coverage of acetylene at 80 K followed by annealing produced ethylidyne by 250 K, with little change in the concentration of this species between 250 and 350 K. They found that following adsorption of a saturation coverage of acetylene at 130 K, ethylidyne was formed only after annealing to 300 K. This difference may be due to the fact that our saturated monolayer after adsorbing at 80 K and annealing to 150 K consisted of a strong mixture of Type I and Type II acetylene, while their saturated monolayer at 130 K consisted almost entirely of Type II acetylene. It is quite possible that these two types of acetylene would undergo slightly different chemistry on clean Ru(001), given that they apparently do so in the presence of a p(2×2) oxygen adatom overlayer.

The mechanism of ethylidyne formation from acetylene on metal surfaces is of considerable importance but has received relatively little attention. We proposed no mechanism in our previous study of acetylene adsorption on clean Ru(001).[2] Jakob et al.[4] recently proposed as a tentative mechanism

$$\mathrm{CHCH(Type\ II)(a)} \xrightarrow[1]{} \mathrm{CCH_2(a)} \xrightarrow[2]{+H} \mathrm{CCH_3(a)}$$

for the decomposition of Type II acetylene on clean Ru(001), where the hydrogen atoms in the second step are provided by the decomposition of additional acetylene molecules to acetylide. At about the same time, Hills[26] independently proposed the similar but slightly more complex mechanism

$$\mathrm{CHCH(a)} \xrightarrow[1]{+H} \mathrm{CHCH_2(a)} \xrightarrow[2]{-H} \mathrm{CCH_2(a)} \xrightarrow[3]{+H} \mathrm{CCH_3(a)}$$
$$\mathrm{CCH_2(a)} \xrightarrow[4]{-H} \mathrm{CCH(a)}$$

In this scheme, the $CHCH_2$ and CCH_2 are viewed as rather unstable reaction intermediates which react quickly to produce one of the two principal products of acetylene decomposition below approximately 350 K, namely ethylidyne and acetylide. The hydrogen atoms in the first step are again produced by the direct decomposition of some acetylene to acetylide. The vinyl ($CHCH_2$) intermediate was invoked primarily for two reasons. First, it avoids the formation of vinylidene via the stable acetylide species (as does the mechanism of Jakob et al.) and also via direct 1,2-hydrogen atom transfer in acetylene. Second, the formation of vinyl from acetylene is very plausible in view of the fact that small amounts of acetylene on Ru(001) can be hydrogenated to ethylene near 175 K in the presence of preadsorbed hydrogen.[3] The experiments with coadsorbed oxygen and acetylene can unfortunately shed little light on to what extent either or both of these mechanisms is operating. The best way to attempt to distinguish between the two is to coadsorb D_2 and C_2H_2 or H_2 and C_2D_2. In the former case, the mechanism of Jakob et al. would produce ethylidyne primarily of the CCH_2D type, while the mechanism of Hills would produce primarily ethylidyne of the $CCHD_2$ type. Our results for C_2H_2 adsorbed on a deuterium presaturated surface and annealed to 300 K[26] show primarily the formation of CCD_2H [$\delta_s(CD_2H)$ = 1150 cm^{-1}] and CCD_3 [$\delta_s(CD_3)$ = 1050 cm^{-1}], with a smaller amount of $CCDH_2$ [$\delta_s(CDH_2)$ = 1260 cm^{-1}] and no CCH_3. While the predominance of CCD_2H is more consistent with the mechanism of Hills, our data base is not extensive, and the mixture of ethylidyne products suggests that more than one mechanism and/or exchange reactions may be occurring. Furthermore, it is possible that the mechanism of ethylidyne formation is altered by the presence of coadsorbed oxygen adatoms. Future investigations along these lines would be of obvious interest.

The products of ethylidyne decomposition on Ru(001) are also controversial, and no fewer than three decomposition reactions have been proposed for ethylidyne decomposition on the clean surface. These are the following:

$$\mathrm{CCH_3(a)} \rightarrow \mathrm{C(a) + CH(a) + 2H(a)}^{8}$$

$$\mathrm{CCH_3(a)} \rightarrow \mathrm{2C(a) + 3H(a)}^{2,12}$$

$$\mathrm{CCH_3(a)} \rightarrow \mathrm{CCH(a) + 2H(a)}^{4}$$

We are currently of the opinion that all of these reactions may occur to some extent, depending on the local concentrations of various surface species, although we still believe that the second is the principal decomposition on clean Ru(001) based on our thermal desorption result for coadsorbed carbon monoxide and ethylene.[13] On Ru(001)-p(2×2)O it is primarily the decomposition of vinylidene (and possibly also acetylide) that correlates with the appearance of the intense δ(CH) mode of methylidyne near 800 cm^{-1} and not the decomposition of ethylidyne. The same appears to be true on Ru(001)-p(1×2)O.

iv. Methylidyne (CH). When acetylene is adsorbed on Ru(001),[2,4] Ru(001)-p(2×2)O or Ru(001)-p(1×2)O and the surface is annealed to temperatures in the range of approximately 400–700 K, at least one hydrocarbon intermediate is formed that is characterized by a strong δ(CH) loss feature near 800 cm^{-1} and a ν(CH) loss feature in the range of 3000–3050 cm^{-1}. The same is true of ethylene adsorption of Ru(001)[8,12] and Ru(001)-p(2×2)O.[9,10] Broad, weak loss features are sometimes present as well between 1000 and 1500 cm^{-1}.[4,12] The hydrogen-containing species was originally assigned by Barteau et al. as a bent methylidyne (CH).[8] We subsequently endorsed this assignment[3,12] and attributed the loss features between 1000 and 1500 cm^{-1} to ν(CC) loss features of carbon dimers.[12] More recently, Jakob et al. have suggested that a number of carbonaceous fragments are present following acetylene decomposition on Ru(001) between 400 and 700 K, possibly including methylidyne, acetylide, and larger species.[4]

While the coexistence of several hydrogen-containing surface species in this temperature range cannot be ruled out (especially since some may be present in very low concentrations), we still favor methylidyne as being the principal hydrogen-containing species present. We have not found the intensity of the δ(CH) mode near 800 cm^{-1} to show much correlation with the weak loss features between 1000 and 1500 cm^{-1}, and occasionally the δ(CH) and ν(CH) loss features are isolated quite cleanly in the absence of these modes [cf. Figure 5g]. We thus prefer to identify these weak features with some (possibly several) forms of surface carbon. We do not believe that the presence of three weak H_2 thermal desorption maxima between 500 and 700 K[3,4] is inconsistent with the presence of only methylidyne and surface carbon, given the possible effects of variations in the local concentrations of these species on the surface and the averaging effects that occur in thermal desorption spectra. Acetylide has a substantially lower frequency CH bending mode (approximately 750 cm^{-1}) than methylidyne and does not appear to be present on either the clean or oxygen-precovered surfaces above 400–450 K. We thus believe, in agreement with our own previous conclusions and those of Barteau et al.,[8] that methylidyne is the principal hydrocarbon species present on the surface between 400 and 700 K.

Methylidyne seems to be formed via the decomposition of several surface species, including acetylide, vinylidene, and (directly or indirectly) ethylidyne on both oxygen-precovered Ru(001) surfaces. Its decomposition is complete near 700 K on both of these surfaces and on clean Ru(001).

V. Summary

Electron energy loss spectroscopy and thermal desorption mass spectrometry have been used to investigate the adsorption and decomposition of acetylene on Ru(001)-p(2×2)O and Ru(001)-p(1×2)O, and the results have been compared to those of previous studies of acetylene on clean Ru(001). The principal

(26) Hills, M. M. Ph.D. Thesis, California Institute of Technology, 1987; pp 154–163.

conclusions of this study are the following.

(1) The saturation coverages of acetylene adsorbed on clean Ru(001), Ru(001)–p(2×2)O, and Ru(001)–p(1×2)O at 80 K are approximately 0.39, 0.31, and 0.09, respectively. These coverages are based on the assumption that the saturation coverage of hydrogen adatoms on Ru(001) following exposure to H_2 at 80 K is 0.85 monolayer.

(2) On Ru(001)–p(2×2)O, as on clean Ru(001),[4] two types of acetylene are formed: Type I at low coverages and Type II at high coverages. On Ru(001)–p(1×2)O only Type II acetylene is formed. This supports the previous suggestion that Type I acetylene adsorbs in μ-sites, since such adsorption sites are available on Ru(001) and Ru(001)–p(2×2)O but not on Ru(001)–p(1×2)O (assuming that preadsorbed oxygen atoms block adjacent 3-fold hollow sites toward the adsorption of acetylene carbon atoms).

(3) The molecularly chemisorbed acetylene species formed on Ru(001)–p(2×2)O and Ru(001)–p(1×2)O are very similar to the corresponding species formed on clean Ru(001), as judged by their EEL spectra. This is in marked contrast to the adsorption of ethylene, which is di-σ-bonded on clean Ru(001) and π-bonded on Ru(001)–p(2×2)O and Ru(001)–p(1×2)O. This difference is probably due to the lower energy of the acetylene π^* orbitals compared to the ethylene π^* orbital. The lower π^* orbital energies in the case of acetylene lead to a nearly sp^3 hybridization of this molecule on all three surfaces.

(4) As on clean Ru(001), chemisorbed acetylene on Ru(001)–p(2×2)O and Ru(001)–p(1×2)O does not desorb molecularly but decomposes completely to yield H_2(g) as the only hydrogen-containing thermal desorption product. Decomposition begins just above 200 K on Ru(001)–p(2×2)O and near 300 K on Ru(001)–p(1×2)O.

(5) As on clean Ru(001), the decomposition of acetylene on the oxygen-precovered surfaces is complex and involves a number of stable intermediates. The reactions may be summarized as follows (these clearly are not intended to represent elementary steps).

Ru(001)–p(2×2)O

$$\text{CHCH (Type II)} \xrightarrow{\sim 200\text{–}300\ \text{K}} \text{CCH} + \text{CCH}_3 + \text{H}$$

(small amounts of CCH_2 and/or $CHCH_2$ are probably also formed)

$$\text{CHCH (Type I)} \xrightarrow{\sim 300\text{–}350\ \text{K}} \text{CCH}_2\ (sp^2)$$

$$\text{CCH,CCH}_2\text{,CCH}_3 \xrightarrow{\sim 350\text{–}450\ \text{K}} \text{CH} + \text{surface carbon} + \text{H}$$

$$\text{CH} \xrightarrow{\sim 500\text{–}700\ \text{K}} \text{surface carbon} + \text{H}$$

$$2\text{H} \xrightarrow{\sim 215\text{–}700\ \text{K}} \text{H}_2\text{(g)}$$

Ru(001)–p(1×2)O

$$\text{CHCH (Type II)} \xrightarrow{\sim 300\text{–}350\ \text{K}} \text{CCH} + \text{CCH}_2 + \text{CCH}_3 + \text{H}$$

$$\text{CCH,CCH}_2\text{,CCH}_3 \xrightarrow{\sim 400\text{–}450\ \text{K}} \text{CH} + \text{surface carbon} + \text{H}$$

$$\text{CH} \xrightarrow{\sim 500\text{–}700\ \text{K}} \text{CH} + \text{surface carbon} + \text{H}$$

$$2\text{H} \xrightarrow{\sim 300\text{–}700\ \text{K}} \text{H}_2\text{(g)}$$

(6) An sp^2-hybridized vinylidene species is formed in especially large amounts on Ru(001)–p(2×2)O from the decomposition of Type I acetylene. Little if any of this vinylidene is formed either on Ru(001)–p(1×2)O (where no Type I acetylene forms) or on clean Ru(001) (where there is no stabilization by coadsorbed oxygen).

Acknowledgment. We gratefully acknowledge the assistance of Dale Johnson in obtaining some of the thermal desorption spectra. This work was supported by the National Science Foundation via Grant no. CHE-8617826.

Registry No. C_2H_2, 74-86-2; O_2, 7782-44-7; Ru, 7440-18-8; CCH_3, 67624-57-1; CCH, 29075-95-4; CH, 3315-37-5; CCH_2, 2143-69-3.